Macromolecules **1999,** *32,* 2221−2231

Atom Transfer Radical Copolymerization of Styrene and *n*-Butyl Acrylate

Stephen V. Arehart and Krzysztof Matyjaszewski*

Department of Chemistry, Carnegie Mellon University, 4400 Fifth Avenue, Pittsburgh, Pennsylvania 15213

Received October 29, 1998; Revised Manuscript Received February 9, 1999

ABSTRACT: Styrene and *n*-butyl acrylate were copolymerized by atom transfer radical polymerization catalyzed by CuBr/4,4′-di(5-nonyl)-2,2′-bipyridine. Composition was consistent with a simple terminal model analysis and was independent of $[\mathrm{CuBr}]_0$, $[\mathrm{I}]_0$, and temperature for copolymerizations with initial feed content of styrene $(f_{\mathrm{st}})_0 = 0.510$. Monomer reactivity ratios evaluated from experimental data by nonlinear least-squares calculations were $0.68 \le r_1 \le 0.82$ and $0.22 \le r_2 \le 0.26$. ^{13}C NMR spectra of styrene/*n*-butyl acrylate copolymers were very similar to copolymers prepared through conventional radical polymerizations, indicating that carbon-centered free radicals were generated under these conditions. Conversion/molecular weight plots showed no evidence of transfer, though measured molecular weights were consistently higher than theoretical ones. Semilogarithmic plots of monomer conversion versus time were nonlinear, indicating an irreversible termination reaction whose contribution decreases with decreasing temperature. Polymerizations of styrene in *n*-butyl propionate (a nonpolymerizable model for *n*-butyl acrylate) were also nonlinear, suggesting that end group decomposition of styrene units was enhanced by the presence of *n*-butyl acrylate.

Introduction

There has been a prolific development of controlled radical polymerization in the past four years. Stable nitroxide radicals have been used to polymerize styrene and its derivatives, and catalysts based on transition metals such as ruthenium, nickel, palladium, and copper have been used to polymerize styrenes, acrylates, methacrylates, and acrylonitrile.[1]

These systems have also been used in simultaneous copolymerizations of vinyl monomers to form statistical copolymers. TEMPO-mediated simultaneous copolymerizations of styrene with chloromethylstyrene,[2] styrene with *n*-butyl acrylate and methyl methacrylate,[3] and styrene with acrylonitrile[4] have been reported. In the latter work, ^{13}C NMR was used to demonstrate that the microstructure in statistical copolymers prepared with TEMPO was very similar to that of statistical copolymers prepared under conventional free radical conditions,[5] indicating that the radicals generated in the two sets of conditions had similar chemoselectivities. Data on copper-catalyzed atom transfer radical polymerization (ATRP) of methyl methacrylate and *n*-butyl methacrylate using Schiff bases as complexing ligands indicate that radicals generated under these conditions also have chemoselectivities similar to those of radicals generated in a conventional process.[6] A very recent report on polymerization of styrene and methyl methacrylate using ruthenium/aluminum complexes also indicates that chemoselectivities of radicals generated are similar to those in a conventional radical polymerization.[7] Preliminary results from our laboratories indicate that it is possible to copolymerize styrene with *n*-butyl acrylate[8] and styrene with acrylonitrile[9] to form copolymers with controlled composition gradients along the chain.[10,11] Kinetic considerations indicate that the composition of statistical copolymers prepared with transition metal complexes should be identical to copolymers prepared under conventional radical polymerization conditions.[12]

Even with such rapid development in controlled radical polymerizations, there are still questions regarding copolymerizations catalyzed by transition metal complexes. Typically, kinetics of homopolymerizations follow a first-order dependence with respect to monomer concentration, though simulations indicate that this is not strictly necessary for these processes.[13] Are the kinetics of simultaneous copolymerization with transition metal complexes more complicated? Do Lewis acidic metal compounds and Lewis basic ligands affect the kinetics, composition, and sequence distribution in these reactions? Do exchange reactions affect the average composition? Simultaneous copolymerization conditions form statistical copolymers with a bivariate distribution of composition and molecular weights.[14] Does the form of this distribution depend on the catalytic system and exchange dynamics? How different is this bivariate distribution from that produced in conventional radical copolymerizations?

This paper reports our experiments on the controlled radical copolymerization of styrene and *n*-butyl acrylate catalyzed by copper(I) bromide/4,4′-di(5-nonyl)-2,2′-bipyridine (dNbpy) in an effort to understand how kinetics, composition, and sequence distribution of copolymerizations depend on transition metal complexes.

Experimental Section

Materials. 2,2′-Azobis(isobutyronitrile) (AIBN, Aldrich, 99%) was recrystallized from methanol below 40 °C and stored cold. *n*-Butyl acrylate (Acros, 99%) was purified by washing with aqueous NaOH, drying over $\mathrm{CaCl_2}$, and distilling under vacuum, collecting the fraction boiling at 72 °C/54 mmHg. Styrene (Acros, 99%) was passed through a column of $\mathrm{Al_2O_3}$ and distilled from $\mathrm{CaH_2}$, collecting the fraction boiling at 68 °C/54 mmHg. All monomers were stored at 0 °C under $\mathrm{N_2}$ in the dark and purged with $\mathrm{N_2}$ for 10 min before use. Experiments at constant initial feed composition were conducted using a solution of styrene and *n*-butyl acrylate mixed in

---

* To whom correspondence should be addressed.

10.1021/ma981693v CCC: $18.00

Table 1. Analysis of Kinetic Samples for Statistical Trends

		styrene			*n*-butyl acrylate			total monomer		
$(f_{st})_0$	conversion	A[a]	s_A	% CV_A	A	s_A	% CV_A	A	s_A	% CV_A
0.132	0.275	2.48	0.07	2.82	25.5	0.8	3.1	28.0	0.9	3.2
	0.681	0.223	0.008	3.6	13.1	0.4	3.1	13.4	0.4	3.0
	0.952	*b*	*b*	*b*	1.80	0.03	1.67	1.80	0.03	1.67
0.510	0.139	21.6	0.6	2.8	17.1	0.4	2.3	38	1	2.6
	0.624	7.1	0.1	1.4	8.4	0.2	2.4	15.4	0.3	1.9
	0.874	1.96	0.05	2.55	3.30	0.08	2.42	5.2	0.1	1.9
0.864	0.074	37	1	3.6	4.6	0.2	4.3	42	1	2.4
	0.687	19.1	0.3	1.6	2.36	0.03	1.27	21.4	0.3	1.4
	0.885	3.82	0.09	2.4	0.375	0.007	1.86	4.2	0.1	2.4

[a] *A* is the ratio of the detector response of the analyte to internal standard. [b] No styrene was detected in this sample.

appropriate proportions and purged with N_2 for 1 h before use. Methyl 2-bromopropionate (Aldrich, 99%) was distilled at reduced pressure, collecting the fraction boiling at 75 °C/58 mmHg. 4-(5-Nonyl)pyridine (Aldrich, 97%) was used without further purification. 4,4′-Di(5-nonyl)-2,2′-bipyridine (dNbpy) was synthesized in 40% yield according to a literature procedure.[15] Copper(I) bromide (CuBr, Aldrich, 99%) was purified by stirring in glacial AcOH for 12 h, filtering, washing with EtOH, and then drying under vacuum at 75 °C/3 days. 1,2-Dichlorobenzene (Aldrich, 99%) was purified by washing with concentrated H_2SO_4 and then washing with distilled water, aqueous $KHCO_3$, and distilled water again. It was dried over $CaCl_2$ and distilled, collecting the fraction boiling at 40 °C/3 mmHg. 1,4-Dimethoxybenzene (Aldrich, 99%) was recrystallized from methanol. Rubber septa (Aldrich) were soaked in THF until the decanted supernatant was colorless and then air-dried. All other solvents and reagents were used without further purification.

Methods. Kinetic measurements were performed on a Shimadzu GC-14A gas chromatograph (GC) using 1,4-dimethoxybenzene as an internal standard. Molecular weights (relative to linear polystyrene standards) were measured using a Waters GPC equipped with 10^2, 10^3, and 10^5 Å PSS columns and a Waters 410 refractive index detector, using 1,2-dichlorobenzene as an internal standard. Data were collected on a Dell Optiplex PC with a 100 MHz Pentium processor and analyzed using PSS 4.0.1 GPC software. ^{1}H NMR spectra were recorded on a Bruker AC 300 (300 MHz) NMR in $CDCl_3$ using TMS as an internal standard. ^{13}C NMR spectra were recorded on an IBM NR/300 equipped with a Bruker 300 MHz magnet and Tecmag data collection software. A pulse delay of 5 s was used to ensure complete relaxation of spins. Copolymerizations were simulated on a Dell Optiplex PC with a 100 MHz Pentium processor using Predici 4.3.9 to determine the cumulative composition dependencies. In selecting monomer reactivity ratios for comparison, the Kelen−Tüdös method was considered an acceptable method of linearization.

Statistical Considerations. Conversion for all copolymerizations was calculated from gas chromatography through eq 1:

$$\text{conversion} = \frac{A_0 - A_t}{A_0} \tag{1}$$

where A_0 represents the detector response ratio of monomer to internal standard at zero time and A_t is this ratio at time *t*. Conversion values presented this way are fractional, ranging from zero to unity. Cumulative copolymer composition of monomer 1($F_{\text{cum, M1}}$) can be calculated from the conversion using eq 2 (assuming that monomer is consumed only in polymerization):

$$F_{\text{cum,M1}} = \frac{\Delta[M_1]}{\Delta\{[M_1] + [M_2]\}} = \frac{[M_1]_0(M_1\ \text{conversion})}{\{[M_1]_0(M_1\ \text{conversion})\} + \{[M_2]_0(M_2\ \text{conversion})\}} \tag{2}$$

where $\Delta[M_1]$ and $\Delta\{[M_1] + [M_2]\}$ are the changes in concentrations of M_1 and M_2. Alternatively, initial moles can be used in place of $[M_1]_0$ and $[M_2]_0$ if the volume of the reaction is not known accurately.

Imprecision in both monomer conversion and calculated copolymer composition arises from imprecision in measuring the response ratio *A*. In copolymerizations it is possible that the imprecision may depend on conversion for a given initial feed and on initial feed conditions. For instance, the percent coefficient of variance of the analyte-to-solvent ratio (% $CV_x = s_x/x \times 100$ where s_x is the standard deviation calculated from a sample of *N* replicate measurements with mean x[16]) of solutions of styrene and 1-vinylimidazole in toluene analyzed by GC depends on the amount of added poly(1-vinylimidazole), with % CV_x for the ratio of 1-vinylimidazole to toluene increasing with increasing polymer content.[17] Therefore, we evaluated our data for any dependence of imprecision on feed conditions and conversions. We selected three samples of low, medium, and high conversion from each of three initial feed conditions and measured the mean detector response for each monomer with 10 replicate injections. The results are shown in Table 1. The mean value of *A* determined from each sample is listed, along with the standard deviation and the % CV_A. This number is useful because it expresses the relative imprecision of *A*. These data show that the imprecision of conversion estimates from GC are independent of conversion for a given initial feed condition (up to 95% conversion) and independent of the initial feed conditions. Therefore, we averaged all the values of % CV_A in Table 1 to obtain a “nominal value” of % $CV_A = 2.0\%$. This value was used for calculating imprecision in conversion and composition for all of our data sets. For instance, knowing % CV_A, the error in conversion can be estimated by combining eq 1 with standard error propagation formulas.[18] The estimated errors are displayed as error bars on kinetic and composition plots.

In some cases, composition obtained from GC is compared with composition measured directly by ^{1}H NMR. For calculating errors in composition from ^{1}H NMR we used eq 3:

$$F_{\text{cum,M1}} = \frac{A_{\text{M1}}}{A_{\text{M1}} + A_{\text{M2}}} \tag{3}$$

where $A_{\text{M1(M2)}}$ is the area of the signal from a well-resolved peak of M_1 (M_2) divided by the number of protons contributing to that signal. Typically, the aromatic region ca. 6.5−7.0 ppm (phenyl ring) is used for styrene, and a broad singlet at ca. 4.0 ppm ($-CO_2CH_2-$ of *n*-butyl acrylate) is used for *n*-butyl acrylate. The normalized areas under both resonances are combined to obtain the denominator in eq 3. A previous study on poly(methyl methacrylate) indicated that the normalized intensity between the backbone $-CH_2-$ and the α-CH_3 had a % CV = 6%.[19] Therefore, we used a % CV_A for $A_M = 6.0\%$ for calculating the error in copolymer composition measured by ^{1}H NMR.

The coefficient of variation for estimating the molecular weight is less than 1%, based on eight replicate injections of a polystyrene sample whose $M_n = (1.10 \pm 0.01) \times 10^4$. The imprecision in measuring molecular weight is very small and is therefore not considered in this paper. However, it is important to remember that all molecular weights of the copolymers are based on polystyrene standards, which will introduce a systematic error in the *accuracy* of the measurement.

Monomer Reactivity Ratios. Low conversion copolymer composition values calculated from residual feed analysis have very large errors (cf. Figures 9 and 10). Additionally, at low conversions composition may be biased by preferential initiation of one monomer by the initiating radical. Therefore, we used our extended conversion kinetic data to estimate monomer reactivity ratios, dictating that an integrated form of the composition equation (such as eq 4) be used to interpret the results:

$$1-\frac{[\mathrm{M}]}{[\mathrm{M}]_0} = 1 - \left(\frac{f_1}{(f_1)_0}\right)^{\alpha}\left(\frac{1-f_1}{1-(f_1)_0}\right)^{\beta}\left(\frac{(f_1)_0-\delta}{f_1-\delta}\right)^{\gamma} \qquad (4)$$

where $1 - [\mathrm{M}]/[\mathrm{M}]_0$ is conversion, f_1 is the feed composition of styrene at that value of conversion, $(f_1)_0$ is the initial feed composition, $\alpha = r_2/(1 - r_2)$, $\beta = r_1/(1 - r_1)$, $\delta = (1 - r_2)/(2 - r_1 - r_2)$, and $\gamma = (1 - r_1r_2)/[(1 - r_1)(1 - r_2)]$. To use eq 4 to determine r_1 and r_2, we used a nonlinear least-squares analysis where the sum of squares of residuals between measured and predicted conversion (eq 5) are minimized by changing r_1 and r_2:

$$\mathrm{SS}(r_1,r_2) = \sum_{i=1}^{n}\frac{1}{w}\{y_i - f(r_1,r_2)_i\}^2 \qquad (5)$$

where y_i is the measured value of conversion at the ith experimental data point, $f(r_1,r_2)_i$ is the value of eq 4 at the ith experimental data point calculated from measured f_1 and $(f_1)_0$, and w is a weighting factor which can be used to account for the error structure of the dependent variable.[20] Statistical calculations on conversion data indicate that the standard deviation of calculated conversion $0.025 \le s_{\mathrm{conv}} \le 0.028$ for all data used for estimating r_1 and r_2. Within the precision of the estimate of this quantity, s_{conv} can be considered constant and $w = 1$ in eq 5 (corresponding to constant absolute error in y).

We realize that there is error in the independent variable (most of which comes from the error in estimating f_1 by GC) which violates an inference assumption in least-squares calculations. (The independent variable has no error.) We initially attempted to use an approximate error-in-variables method (EVM) for our calculations,[21] but our estimates for the Hessian matrix were unreliable, producing joint confidence intervals (JCIs) that were too small.

For our least-squares procedure, we opted to use the “sum-of-squares space” (SS space) approach,[20,22] which is less likely to converge to a local minimum. (The surface is inspected visually.) Adapting this approach to our calculations, the JCI is calculated from eq 6:

$$\mathrm{SS}(r_1,r_2) \le \mathrm{SS}(\hat{r}_1,\hat{r}_2) + \sigma^2\chi^2_{0.95;2} \qquad (6)$$

where $\mathrm{SS}(r_1,r_2)$ is the value of eq 5 at a given r_1,r_2 value, $\mathrm{SS}(\hat{r}_1,\hat{r}_2)$ is the value of eq 5 at the point estimates for the monomer reactivity ratios, and $\sigma^2\chi^2_{0.95;2}$ is the product of the variance of monomer conversion (estimated to be 9×10^{-4} for our reactions) and the chi-squared parameter at the 95% confidence interval for 2 degrees of freedom. To construct the SS space, eq 5 was evaluated for a range of r_1 and r_2 values for a given data set in Excel 7.0 using a looping structure written in an Excel Visual Basic for Applications (VBA) module. Full details of the calculations as well as the complete VBA code used to construct the SS space surface are available in the Supporting Information. Our results are displayed as JCIs of r_2 versus r_1.

Simultaneous Atom Transfer Radical Copolymerizations. Simultaneous copolymerizations of styrene and *n*-butyl acrylate for kinetic measurements were performed as in the following. In a typical procedure, CuBr (55 mg, 0.4 mmol), dNbpy (0.32 g, 0.8 mmol), and 1,4-dimethoxybenzene (0.14 g, 1 mmol) were placed in a round-bottom flask with a rubber septum and stir bar. The solids were evacuated and backfilled three times with N_2. A solution of styrene and *n*-butyl acrylate (4.6 g of solution, 0.02 mol of styrene, 0.02 mol of *n*-butyl acrylate) and then methyl 2-bromopropionate (66 mg, 0.4 mmol) were added via syringe. A 100 μL aliquot was removed from the reaction, and the reaction was heated at 90 °C for 24 h. Aliquots (150 μL) were removed from the reaction at 300, 900, 1200, 1920, 3660, 5400, 7200, and 10 870 s. The aliquots were divided between two sets of vials. One set was diluted with THF (ca. 2 mL) and analyzed by GC. 1,2-Dichlorobenzene (ca. 0.5 mL) was added to these samples, and they were filtered through a small plug of Al_2O_3 then a 0.2 μm filter and analyzed by GPC. The second set was diluted in $CHCl_3$ and filtered through a small plug of Al_2O_3. The solvent was evaporated at room temperature, and the samples were redissolved in $CDCl_3$ and analyzed by ^{1}H NMR.

Table 2. Reaction Conditions for Statistical Copolymerizations of Styrene and *n*-Butyl Acrylate at 110 °C

experiment	$(f_{\mathrm{st}})_0$	$[\mathrm{M}]_0$:$[\mathrm{I}]_0$:$[\mathrm{CuBr}]_0$:$[\mathrm{dNbpy}]_0$
1	0.132	100:1.0:1.0:2.0
2	0.132	101:1.0:1.0:2.0
3	0.132	100:1.0:1.0:2.0
4	0.510	100:1.0:1.0:2.0
5	0.510	100:1.0:1.0:2.0
6	0.510	99:1.0:1.0:2.0
7	0.864	100:1.0:0.9:1.8
8	0.864	101:1.0:0.9:1.8
9	0.864	101:1.0:1.0:2.0
10	0.741	102:1.0:1.1:2.2
11	0.258	101:1.0:2.1
12[a]	0.510	101:1.0:1.0:2.0

[a] 70 °C.

Synthesis of Poly(styrene-*stat*-*n*-butyl acrylate) by Conventional Radical Polymerization. Styrene (6.0 g, 0.06 mol), *n*-butyl acrylate (7.3 g, 0.06 mol), AIBN (0.3 g, 2 mmol), carbon tetrabromide (11 mg, 3×10^{-5} mol), and benzene (30 mL) were combined in a 50 mL Schlenk flask with a N_2 inlet−outlet and rubber septum. The reaction was degassed with three freeze−pump−thaw cycles (total pump time = 0.5 h) and then heated at 60 °C for 24 h, at which point the reaction had reached 77% total monomer conversion. The polymer was precipitated in methanol (600 mL) and water (50 mL). The supernatant was decanted, leaving a gummy, very viscous polymer. This was washed several times with methanol and then dried under vacuum at 75 °C for 14 h to yield 4.6 g (35%) of poly(styrene-*stat*-*n*-butyl acrylate) as a clear, amorphous polymer: $M_{\mathrm{n}} = 2.3 \times 10^4$, $M_{\mathrm{w}}/M_{\mathrm{n}} = 1.62$, $F_{\mathrm{styrene}} = 0.58$.

Chain Extension of Poly(styrene-*stat*-*n*-butyl acrylate) by ATRP. CuBr (13 mg, 0.1 mmol), dNbpy (0.08 g, 0.2 mmol), and 1,4-dimethoxybenzene (0.13 g, 1 mmol) were placed in a round-bottom flask with a rubber septum and stir bar. The solids were evacuated and backfilled three times with N_2. A 25 wt % solution of macroinitiator ($M_{\mathrm{n}} = 1.2 \times 10^4$, $M_{\mathrm{w}}/M_{\mathrm{n}} = 1.13$) in styrene (3.9 g, 0.03 mol of styrene, 0.1 mmol of macroinitiator) was added via syringe. A 100 μL aliquot was removed from the reaction, and the reaction was heated at 110 °C for 10 h. Samples were removed at 4200, 12 420, and 20 280 s. The samples were placed in vials and diluted with THF (ca. 2 mL) and analyzed by GC. 1,2-Dichlorobenzene (ca. 0.5 mL) was added to these samples, and they were filtered through a small plug of Al_2O_3 and then a 0.2 μm filter and analyzed by GPC.

Results and Discussion

Copolymerization Kinetics. Figures 1 and 2a−c plot ln $[\mathrm{M}]_0/[\mathrm{M}]$ versus time (s) for statistical copolymerizations of styrene and *n*-butyl acrylate. Reaction conditions are shown in Table 2. Absolute volumes were not measured with precision in these reactions, and the data in Table 2 are presented only as molar ratios in

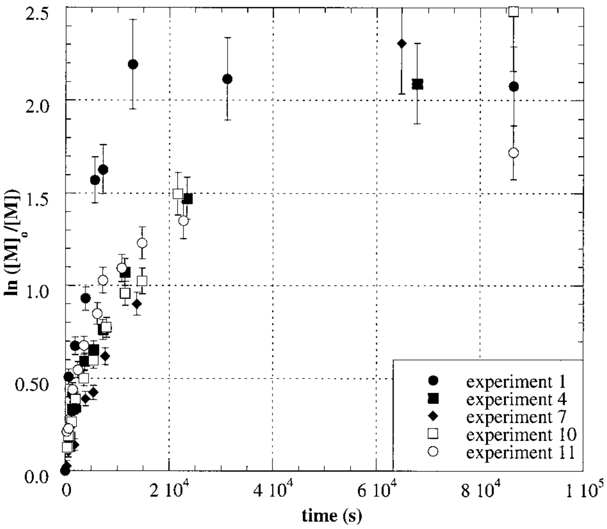

Figure 1. Semilogarithmic kinetic plots for the simultaneous copolymerization of styrene and *n*-butyl acrylate for different initial mole fractions of styrene $(f_{st})_0$. Reaction numbers listed in the legend correspond to conditions in Table 2.

initial conditions. Figure 1 shows kinetic data for five different feed ratios of styrene at 110 °C. Figure 2a–c shows multiple data sets collected for three of the five different feed ratios under identical conditions. The results for each different feed ratio are experimentally identical, showing that the kinetic behavior is reproducible under these conditions.

Figures 1 and 2a–c indicate that atom transfer copolymerizations terminate irreversibly during polymerization, the contribution of which increases with increasing styrene content. This is strange, considering that homopolymerizations of styrene[23] are controlled under similar conditions at 110 °C, and polymerizations of *n*-butyl acrylate under comparable catalyst conditions are controlled at 90 °C.[24] Figure 3 shows that as temperature for copolymerizations with $(f_{st})_0 = 0.510$ is lowered, kinetic plots straighten out, and the correlation coefficients ("*r* values", listed in the figure caption) approach values typical for a completely linear relationship in which the variation in *y* is due completely to variation in *x* (i.e., $r = 1.0$).

What is the side reaction? There are documented reports of elimination of HBr in model reactions of copper bromide/substituted bipyridine salts and 1-phenylethyl bromide, with "fast formation of styrene" in polar solvents such as acetonitrile and nitromethane.[25] Figure 4 shows that polymerizations of styrene in *n*-butyl propionate (a nonpolymerizable model of *n*-butyl acrylate) are also nonlinear, indicating that *n*-butyl acrylate may act as a polar medium, accelerating end group decomposition.

How much functionality is maintained at 110 °C? Figure 5 shows GPC elugrams for a chain extension of poly(styrene-*stat*-*n*-butyl acrylate) synthesized under conditions similar to experiments 4–6 in Table 2 but stopped at 78% total monomer conversion. (The macroinitiator was passed through a small plug of Al_2O_3 to remove catalyst but was not precipitated, since it is not known if precipitation can lead to end group loss.) In trace a, the detector response at the *i*th elution volume has been divided by the molecular weight at the *i*th elution volume to give a trace representative of the *mole fraction (not weight fraction)*[26] of chains of different

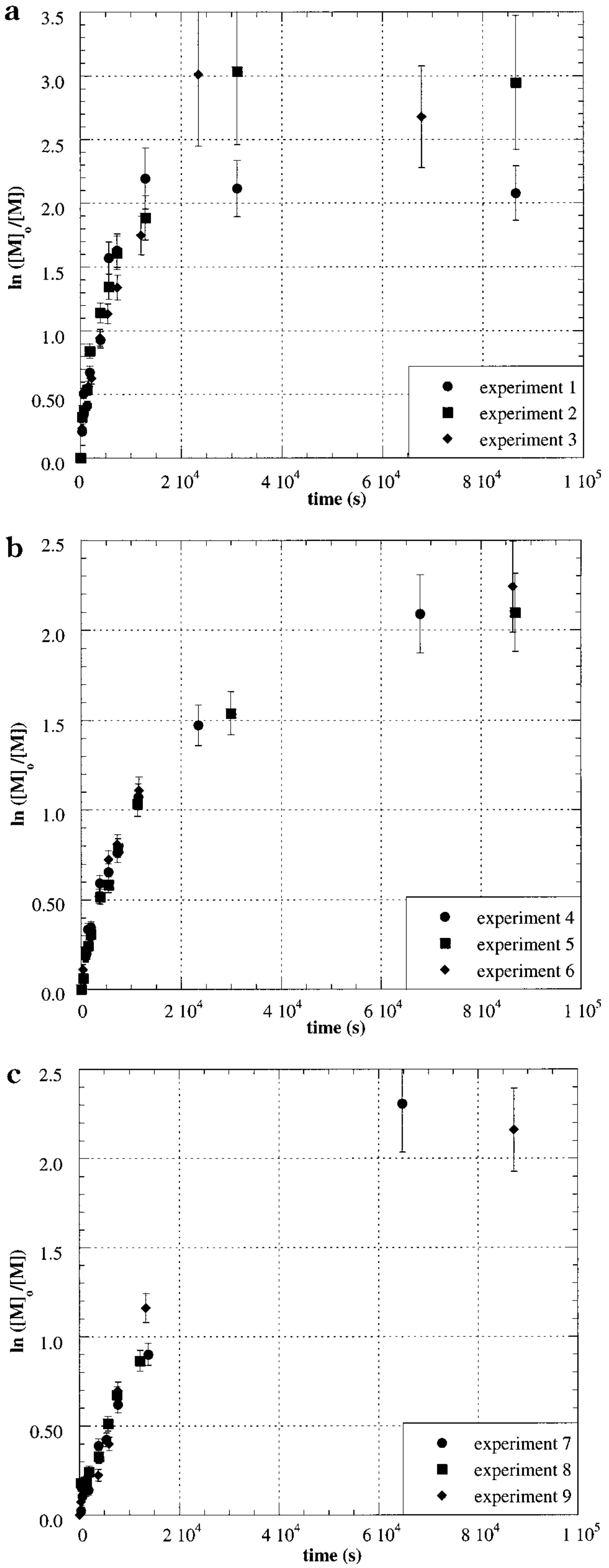

Figure 2. (a) Semilogarithmic kinetic plots for the simultaneous copolymerization of styrene and *n*-butyl acrylate at 110 °C for $(f_{st})_0 = 0.132$. Reaction numbers listed in the legend correspond to conditions in Table 2. (b) Semilogarithmic kinetic plots for the simultaneous copolymerization of styrene and *n*-butyl acrylate at 110 °C for $(f_{st})_0 = 0.510$. Reaction numbers listed in the legend correspond to conditions in Table 2. (c) Semilogarithmic kinetic plots for the simultaneous copolymerization of styrene and *n*-butyl acrylate at 110 °C for $(f_{st})_0 = 0.864$. Reaction numbers listed in the legend correspond to conditions in Table 2.

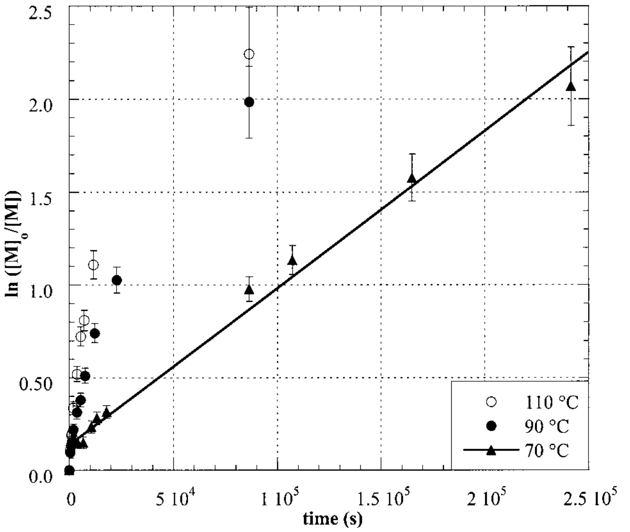

Figure 3. Semilogarithmic kinetic plots for the simultaneous copolymerization of styrene and *n*-butyl acrylate at different temperatures with $(f_{st})_0 = 0.510$. $r_{110\,°C} = 0.84$, $r_{90\,°C} = 0.92$, and $r_{70\,°C} = 0.99$.

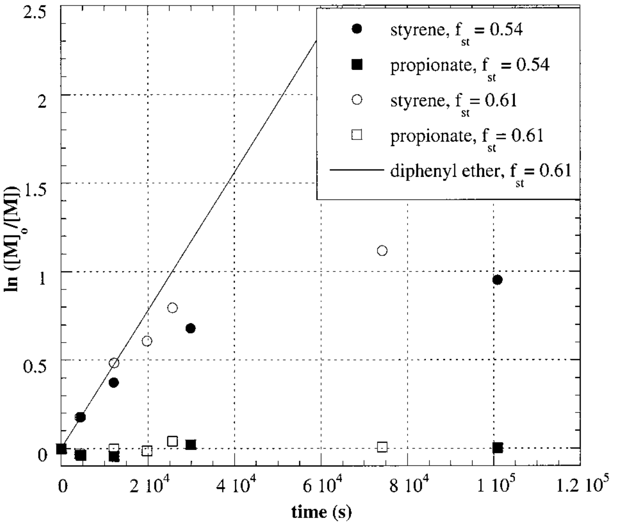

Figure 4. Semilogarithmic kinetic plots for the polymerization of styrene in *n*-butyl propionate at 110 °C at two different contents of styrene. The solid line denotes the measured rate for a solution polymerization of styrene in diphenyl ether.[23]

molecular weight in the sample. Figure 5 shows that there are still a significant number of chains active after extension at 78% conversion but that some chains have died, consistent with the kinetic plots. Trace b shows the detector response versus elution volume without correcting for the molecular weight dependence of the detector response. Without this correction, it is easy to misinterpret the results of chain extensions as a test for functionality, since in this form it appears that there are relatively few dead chains.

What is most important is the relative contribution of this side reaction to the overall controlled nature of the copolymerization. Even with this irreversible termination reaction, polymers with controlled molecular weights (see below) and polydispersities around 1.10 can still be prepared. Additionally, copolymers with molecular weights as high as 5.4×10^4 are prepared with this catalytic system in this paper. Data in Figure 3 suggest that functionality can be increased by lowering polymerization temperatures. Therefore, if high functionality is needed, reaction conditions should be kept at lower temperatures. If the desire is simply to make a predetermined molecular weight, narrow molecular weight distribution copolymer, functionality can be sacrificed for reaction rate at higher temperatures without significantly affecting polydispersity.

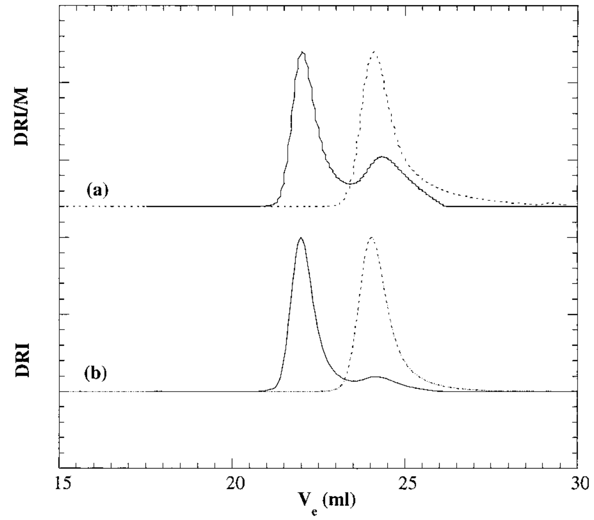

Figure 5. (a) Differential refractive index detector response divided by molecular weight (DRI/*M*) versus elution volume (V_e) for the chain extension of poly(styrene-*stat*-*n*-butyl acrylate) with styrene by ATRP at 110 °C. Dashed line is the macroinitiator, and the solid line is the chain-extended product. (b) Differential refractive index detector response (DRI) versus elution volume (V_e) for the chain extension of poly(styrene-*stat*-*n*-butyl acrylate) with styrene by ATRP at 110 °C. Dashed line is the macroinitiator, and the solid line is the chain-extended product.

Though chain extensions show that curvature in kinetic plots in these reactions is probably due to functionality loss, it is possible that kinetics in copolymerizations proceeding through this mechanism are inherently nonlinear. As feed composition drifts due to preferential consumption of one monomer, the deactivator concentration may change, resulting in a slower overall rate if the monomer left in the feed polymerizes under different equilibrium conditions. For instance, the equilibrium constant K for a bulk styrene polymerization with $X_{n,\mathrm{th}} = 100$ is $K = 6 \times 10^{-8}$ at 100 °C; for *n*-butyl acrylate it is $K = 6 \times 10^{-9}$ at 100 °C.[24] This means that more deactivator ($CuBr_2$) is generated in a styrene polymerization. Forming this amount of deactivator in the presence of *n*-butyl acrylate may slow the consumption of *n*-butyl acrylate during the polymerization, giving rise to nonlinear kinetics which are not due to irreversible destruction of end groups. However, for our case it is difficult to discern the contribution of this proposed mechanism to the overall kinetics.

Molecular Weights. In a polymerization with fast initiation and no chain transfer, all chains begin growth simultaneously, and their number is fixed throughout the polymerization. Therefore, $X_n = \Delta[M]/[I]_0$, and a plot of X_n versus conversion is linear. Normally, the number-average molecular weight (M_n) is used instead, since M_n is measured directly. M_n and X_n are related by eq 7:

$$M_n = M_0 X_n + M_{eg} \tag{7}$$

where M_0 is the mean molecular weight of a structural unit (same as the monomer molecular weight for vinyl polymerizations) and M_{eg} is the mass of the end groups.

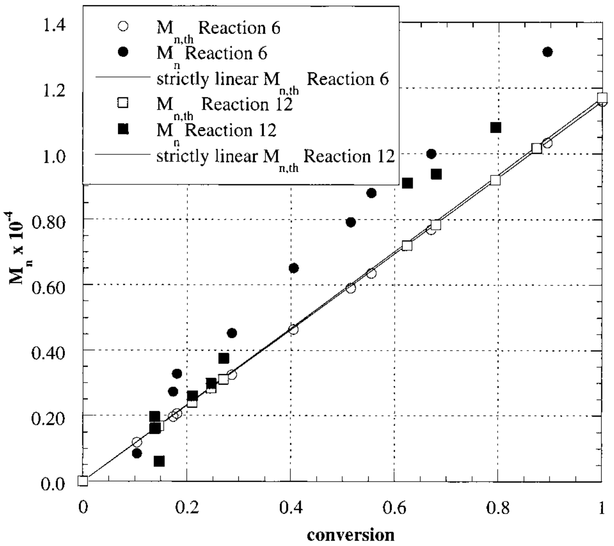

Figure 6. $M_{n,th}$ and M_n versus conversion for the simultaneous copolymerizations of styrene and *n*-butyl acrylate. Reaction numbers listed in the legend correspond to those in Table 2.

In copolymerizations, the situation is more complex since M_0 is a function of composition and therefore conversion. In a copolymerization of two monomers M_0 is given by eq 8:

$$M_0 = A_1F_1 + A_2F_2 \tag{8}$$

where A_1 and A_2 are the molecular weights of M_1 and M_2, respectively, and F_1 and F_2 are the mole fractions of M_1 and M_2 in the polymer, respectively. Therefore, if the mass of monomers is significantly different, one will observe a nonlinear relationship between molecular weight and conversion, even if no transfer occurs during the polymerization.

Figure 6 plots M_n and $M_{n,th}$ versus conversion for statistical copolymerizations of styrene and *n*-butyl acrylate at 110 and 70 °C (experiments 6 and 12 in Table 2). Results shown here are typical for all polymerizations studied in this paper. Theoretical molecular weights, based on combining eqs 7 and 8 and a strictly linear relationship, are both plotted against the measured data for comparison. Figure 6 shows that the influence of different monomer molecular weights on the theoretical molecular behavior is very small, and theoretical molecular weights are well-described by a linear relationship. Figure 6 also shows that measured molecular weights in copolymerizations are slightly higher than either theoretical dependence, suggesting either inefficient initiation or termination by combination, a dominant mode of termination for both polystyryl and polyacrylate radicals.[27] Since molecular weight behavior is similar for copolymerizations at 110 and 70 °C, radical–radical termination is probably not responsible for the increase in molecular weight relative to the theoretical dependence, suggesting inefficient initiation as the primary cause for disagreement. However, *tert*-butyl bromopropionate efficiently initiates polymerization of styrene,[28] and methyl 2-bromopropionate efficiently initiates polymerization of *n*-butyl acrylate.[29] Figure 7 shows a copolymerization with theoretical $X_n = 600$. The disagreement between theoretical and measured molecular weights reaches a maximum around 2.5×10^4 and remains constant up to the final molecular weight of 5.6×10^4. Although this is unusual, it is possible that the intrinsic viscosity [η] of these copolymers (and therefore the hydrodynamic volume) has a molecular weight dependence different from linear polystyrene. Therefore, we attribute the disagreement primarily to differences in hydrodynamic volumes between the polystyrene standards and the copolymer samples.

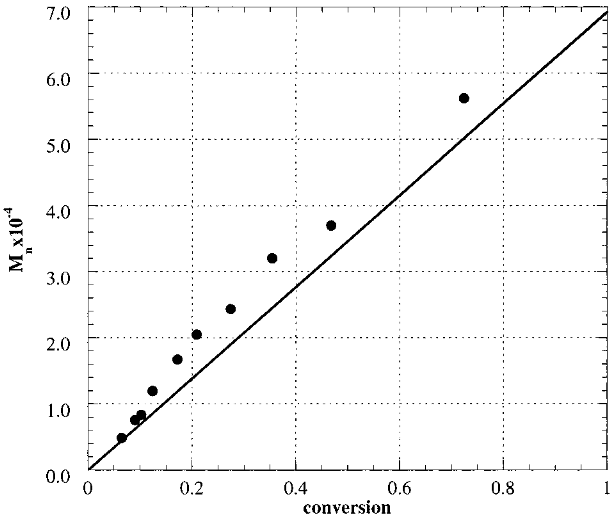

Figure 7. M_n and $M_{n,th}$ versus conversion for simultaneous copolymerizations with $[M]_0:[I]_0:[CuBr]_0:[dNbpy]_0 = 600:1.0:1.0:2.0$ at 90 °C.

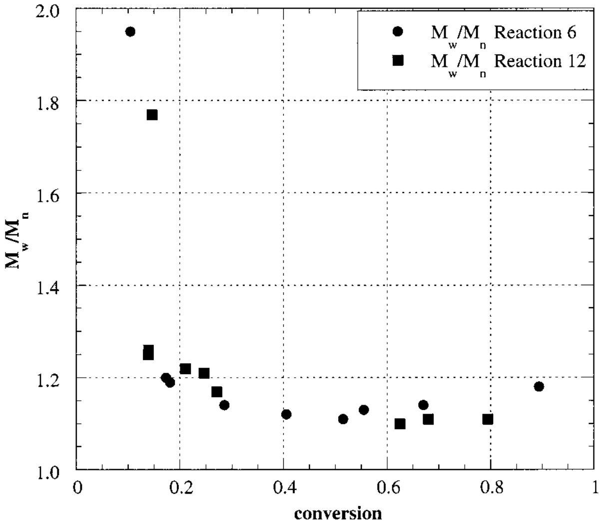

Figure 8. M_w/M_n versus conversion for simultaneous copolymerizations of styrene and *n*-butyl acrylate. Reaction numbers listed in the legend correspond to those in Table 2.

Figure 8 shows M_w/M_n versus conversion for the simultaneous copolymerizations at 110 and 70 °C. Polydispersities in these reactions remain quite low until high conversions, where they increase slightly. (The very high polydispersities at very low conversions are inflated since the calculation of molecular weight includes ligand which cannot be efficiently separated from oligomers on the columns.) These results are also typical for all copolymerizations studied in this paper. Notice that even though there is termination in the kinetic plots at 110 °C, polydispersities for this reaction are below 1.2 and as low as 1.1, emphasizing that polydispersity alone is a poor criterion for judging the living character of a polymerization.[30,31]

Copolymer Composition. Composition is an important element in copolymerizations since it can be used

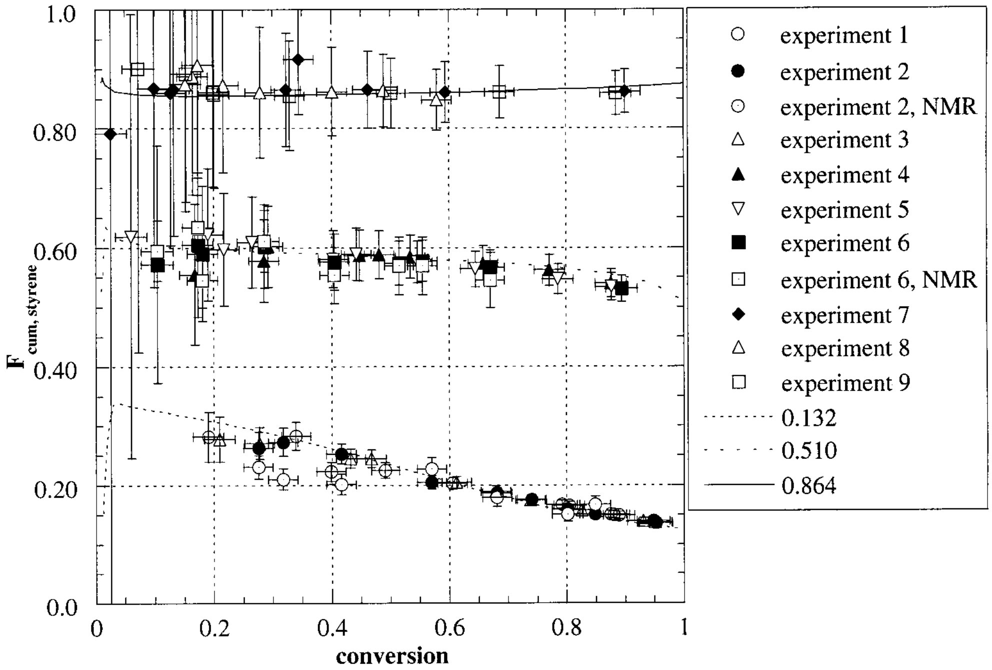

Figure 9. $F_{cum,styrene}$ versus conversion for simultaneous copolymerizations of styrene and *n*-butyl acrylate at 110 °C. Reaction numbers listed in the legend correspond to conditions in Table 2. Lines indicate the theoretical dependencies simulated with Predici using Scheme 1 and rate constants listed in Table 3. Each number for the theoretical line corresponds to the initial styrene feed ($(f_{st})_0$) in the simulation.

Scheme 1. Reaction Scheme Used for Simulating Copolymerizations; Values for Rate Constants Are Listed in Table 3

$$R + M_1 (M_2) \xrightarrow{k_i} P_1 (Q_1)$$

$$P_s + M_1 \xrightarrow{k_{11}} P_s$$

$$P_s + M_2 \xrightarrow{k_{12}} Q_s$$

$$Q_s + M_2 \xrightarrow{k_{22}} Q_s$$

$$Q_s + M_1 \xrightarrow{k_{21}} P_s$$

Table 3. Composition Simulation Rate Constants

reaction	rate constant	value at 50 °C (L mol^{-1} s^{-1})
initiation	k_i	1.0×10^6
styrene homopropagation	k_{11}	2.4×10^2
styrene cross-propagation	k_{12}	3.4×10^2
n-butyl acrylate homopropagation	k_{22}	2.7×10^4
n-butyl acrylate cross-propagation	k_{21}	1.6×10^5

to obtain information on the chemoselectivity of active sites consuming monomer during polymerization. Figure 9 shows the predicted and measured styrene cumulative copolymer composition ($F_{cum,styrene}$) versus conversion for nine of the 12 different simultaneous copolymerizations listed in Table 2. Predicted values were calculated from Predici using the kinetic equations outlined in Scheme 1 combined with rate constants listed in Table 3. Rate constants were calculated by combining reactivity ratios ($r_1 = 0.698$, $r_2 = 0.164$ at 50 °C)[32] with homopropagation rate constants for styrene[33] and *n*-butyl acrylate[34] at 50 °C. This analysis corresponds to a terminal model with fast initiation and can be thought of as the integrated solution of the terminal model composition equation. Most experimental values were calculated from residual feed analysis by gas chromatography using eq 2 (see Experimental Section), but some were also calculated from ^{1}H NMR data using eq 3. Figure 9 shows that for these copolymerizations simulated and measured cumulative copolymer compositions are identical within experimental error, indicating that the active species formed in ATRP have chemoselectivity similar to carbon-centered free radicals generated in a conventional radical copolymerization. Additionally, composition calculated from residual feed analysis is similar to composition measured by ^{1}H NMR, indicating that eq 2 is valid and that monomer is consumed only in polymerization.

Figure 10 shows $F_{cum,\ styrene}$ versus conversion for many different copolymerizations at constant initial styrene feed ($(f_{st})_0 = 0.510$), the reaction conditions for which are summarized in Table 4. Figure 10 shows that $F_{cum,\ styrene}$ is independent of temperature, initiator concentration, and catalyst concentration. The independence of composition on catalyst and initiator concentration is consistent with a reaction proceeding through carbon-centered free radicals where the transition metal complex acts only to catalyze the exchange process and does not interact with the radicals enough to influence their chemoselectivity. The independence of composition on temperature is probably a fortuitous cancellation of different activation energies since ratios are being compared. The temperature (in)dependence of reactivity ratios has been reported very recently for styrene and methyl methacrylate.[35]

Monomer Reactivity Ratios. To quantify the similarity between chemoselectivity of radicals generated in ATRP and conventional copolymerizations, we calculated the monomer reactivity ratios from kinetic data. According to Behnken[36] and Tidwell and Mortimer,[37] optimum feed compositions for measuring monomer reactivity ratios of styrene and *n*-butyl acrylate (based on initial estimates of $r_1 = 0.698$ and $r_2 = 0.164$) are $(f_{st})_0 = 0.10$ and $(f_{st})_0 = 0.75$. We used $(f_{st})_0 = 0.132$ and $(f_{st})_0 = 0.864$ for calculating monomer reactivity ratios. (The higher styrene content was used since the integrated form of the composition equation would return

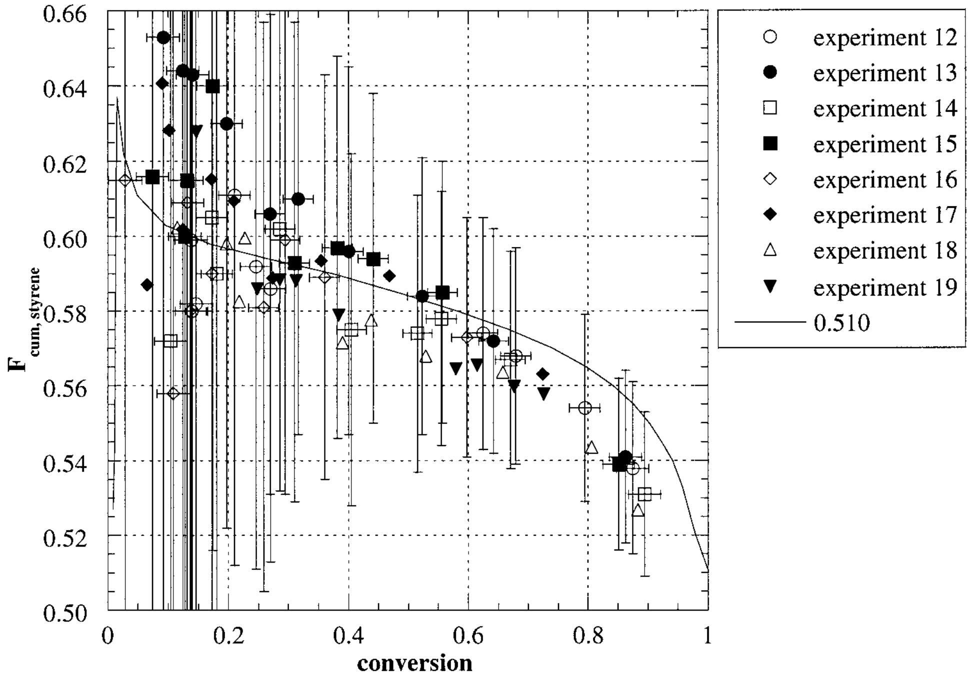

Figure 10. $F_{cum,styrene}$ versus conversion for simultaneous copolymerizations of styrene and *n*-butyl acrylate at $(f_{st})_0 = 0.510$. Reaction numbers listed in the legend correspond to conditions in Table 4. The line indicates the theoretical dependencies simulated with Predici using Scheme 1 and rate constants listed in Table 3.

Table 4. Reaction Conditions for Composition Comparison with $(f_{st})_0 = 0.510$

experiment	$[M]_0:[I]_0:[CuBr]_0:[dNbpy]_0$	temp (°C)
12	101:1.0:1.0:2.0	70
13	100:1.0:1.0:2.0	90
14	99:1.0:1.0:2.0	110
15	300:1.0:3.1:6.2	110
16	300:1.0:3.0:6.0	90
17	600:1.0:5.9:12	110
18	99:1.0:0.8:1.5	110
19	101:1.0:1.5:3.0	110

Table 5. Reactivity Ratios Calculated Using the Kinetic Data from Reactions 1−3 and 7−9 in Table 2

	expt 1	expt 2	expt 3
expt 7	$r_1 = 0.80$; $r_2 = 0.26$	$r_1 = 0.80$; $r_2 = 0.22$	$r_1 = 0.80$; $r_2 = 0.22$
expt 8	$r_1 = 0.68$; $r_2 = 0.25$	$r_1 = 0.67$; $r_2 = 0.22$	$r_1 = 0.67$; $r_2 = 0.23$
expt 9	$r_1 = 0.82$; $r_2 = 0.26$	$r_1 = 0.82$; $r_2 = 0.22$	$r_1 = 0.82$; $r_2 = 0.23$

undefined values at $(f_{st})_0 = 0.75$ with the initial r_1/r_2 estimates.) Experiments 1−3 and 7−9 from Table 2 were combined as shown in Table 5 to give nine different data sets from which monomer reactivity ratios were estimated. Each row in Table 5 represents an experiment with $(f_{st})_0 = 0.864$, and each column represents an experiment with $(f_{st})_0 = 0.132$. As discussed in the Experimental Section, a nonlinear least-squares routine implemented in Excel 7.0 was used for calculating r_1 and r_2 using the "sum-of-squares space" (SS space) approach published previously.[20,22] In filtering a data set to use for analysis, total monomer conversion data less than 20% and higher than 85% were omitted from the analysis. (Low conversion data were omitted since the relative error in conversion is larger at low conversions. High conversion data were omitted since most monomer is consumed at this stage, providing little information on chemoselectivity.)

Figure 11 shows the 95% JCIs constructed from several analyzed data sets using the JCI condition in eq 6. The shape of the JCIs is fairly ellipsoidal for experiments where $(f_{st})_0 = 0.864$ (experiments 7−9), but the exact shape varies according to the experiment used. There are two characteristics of the experimental data which may explain the shape variation. First, in experiment 7 one additional point was eliminated from the analysis since it contributed much more to the total least-squares sum than the others (thus unfairly biasing the point estimate). Second, experiment 8 contained one more conversion data point than did experiments 7 and 9. As pointed out previously, evaluating a surface visually for minima is an old concept[20,22] which has not been economic until now since computers were so slow. Historically, iterative methods have been used to find a point estimate, and how the *surface* (not the point estimates) depends on the data set error structure and initial conditions has not been extensively studied. Therefore, it is difficult for us to quantitatively explain how the JCIs should depend on our experimental data since this depends on the data set error structure, the number of points in the data set, and the fitting equation.

Table 5 shows that $0.68 \leq r_1 \leq 0.82$ and $0.22 \leq r_2 \leq 0.26$. Experiments where $(f_{st})_0 = 0.864$ dominate in the estimate of r_1 whereas experiments where $(f_{st})_0 = 0.132$ dominate the estimate of r_2. Our estimates are consistent with monomer reactivity ratios collected from other sources (Table 6).

Sequence Distribution. Sequence distribution is quite useful for investigating potential polymerization mechanisms, since it can discriminate between copolymerization models much better than composition. However, sequence distribution is also very hard to quantitatively and unambiguously assign.[38] Therefore, the results presented here are qualitative.

Figure 12 shows a typical ^{13}C NMR spectrum recorded for poly(styrene-*stat*-*n*-butyl acrylate) prepared by ATRP. This spectrum is similar to that reported previously for poly(styrene-*stat*-*n*-butyl acrylate) prepared by conventional radical polymerization.[39,40] The region around 175 ppm is relatively free of *stereochemical* effects which

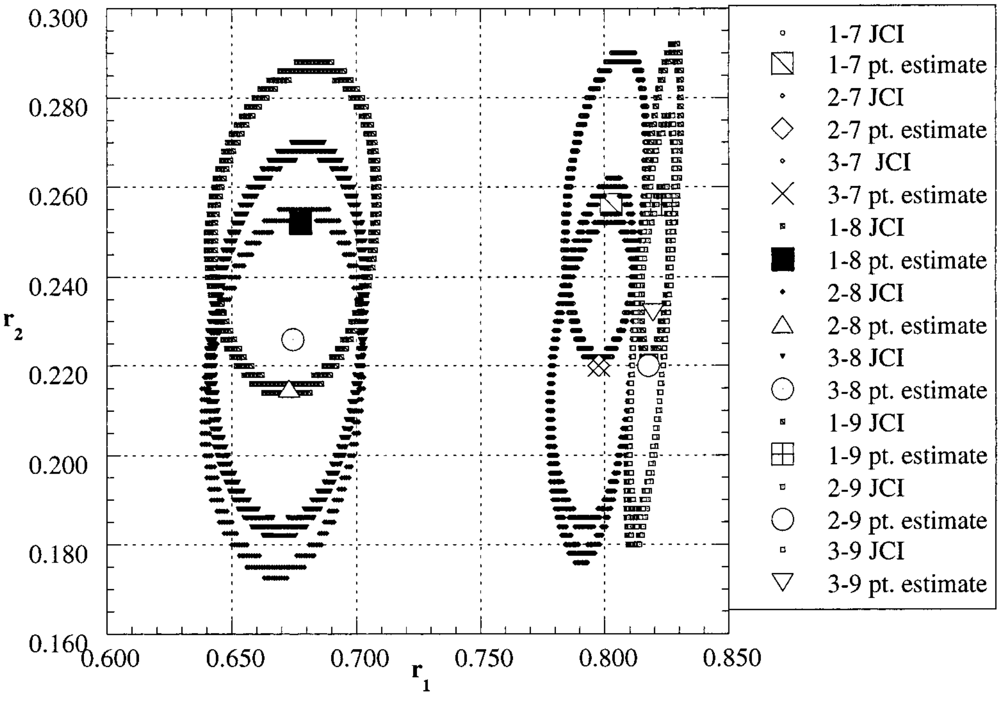

Figure 11. The 95% joint confidence intervals constructed from the SS space calculations for nine different experimental data set combinations derived from combining $(f_{st})_0 = 0.132$ and $(f_{st})_0 = 0.864$ experiments in Table 2 (experiments 1−3 and 7−9). Each reactivity ratio estimate corresponds to combining one low styrene and one high styrene data set. The numbers in the legend correspond to the experiments combined together, the conditions for which are listed in Table 2. "Pt. estimate" indicates the reactivity ratio point estimate derived from the calculations.

Table 6. Monomer Reactivity Ratios of Styrene (r_1) and *n*-Butyl Acrylate (r_2) from Various Sources

method	r_1	r_2	temp (°C)	ref
Kelen−Tüdös[a]	0.698 ± 0.033	0.164 ± 0.017	50	32
EVM[a]	1.21 ± 0.21	0.17 ± 0.07	70	40
EVM	0.955	0.183	50	41
Kelen−Tüdös[a]	0.883	0.207	80	42
Mayo−Huglin[b]	1.006	0.232	80	42
SS space[c,d]	$0.68 \le r_1 \le 0.82$	$0.22 \le r_2 \le 0.26$	110	this work

[a] Below 15% monomer conversion. [b] Above 15% monomer conversion. [c] 25−85% monomer conversion. [d] Range of values corresponds to 95% JCI.

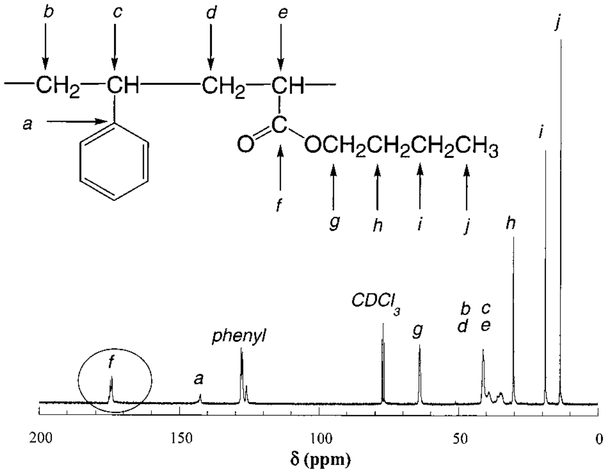

Figure 12. A typical ^{13}C NMR spectrum of poly(styrene-*stat*-*n*-butyl acrylate) prepared by ATRP ($f_{st} = 0.25$).

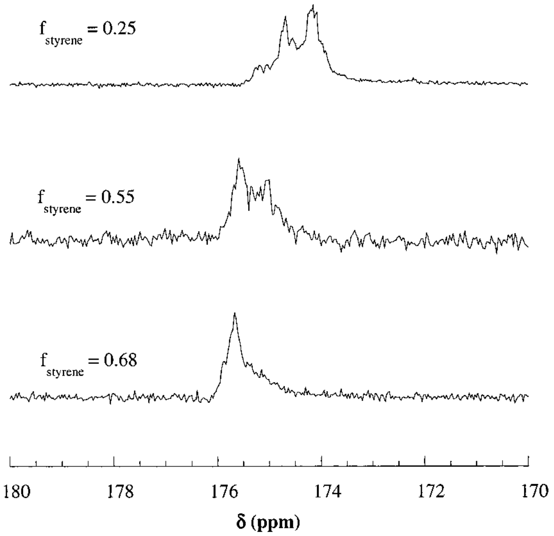

Figure 13. ^{13}C NMR spectra of poly(styrene-*stat*-*n*-butyl acrylate) copolymers prepared by ATRP, showing that the region around 175 ppm is sensitive to composition.

may extend to the pentad level.[39] Therefore, this region will not be complicated by stereochemical effects and can be used to compare copolymers prepared by ATRP and conventional radical polymerization in more detail. Figure 13 shows three copolymers prepared by ATRP with different compositions. Conditions used to prepare these polymers are listed in Table 2. As the amount of styrene increases, broadening of the high field side of the signal increases and the whole signal shifts to higher field, consistent with an electron-withdrawing effect of the phenyl ring on styrene. These results are consistent with what has been reported for poly(styrene-*stat*-*n*-butyl acrylate) prepared by conventional radical polymerization.[39]

Figure 14 compares copolymers synthesized by ATRP and conventional free radical techniques using carbon tetrabromide to limit molecular weight. To ensure

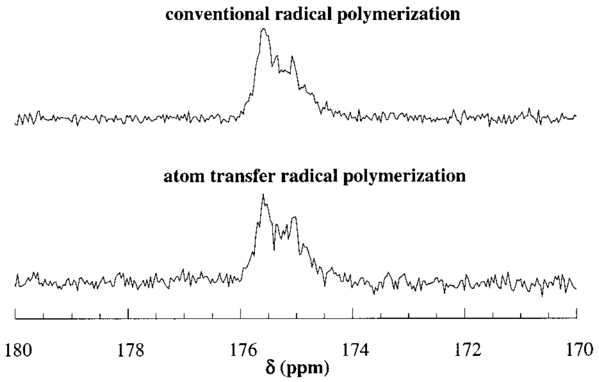

Figure 14. Comparison of the region around 175 ppm between ATRP and conventional free radical poly(styrene-*stat*-*n*-butyl acrylate).

maximum comparability between the two samples, initial feed compositions were the same ($(f_{st})_0 = 0.50$), final average compositions were similar ($f_{st} = 0.57$ for the conventional copolymer and $f_{st} = 0.51$ for the ATRP copolymer), and molecular weights of the two isolated polymers are also similar (2.3×10^4 for the conventional copolymer and 2.1×10^4 for the ATRP copolymer). Figure 14 shows that the sequence distribution in these two copolymers is very similar, suggesting that carbon-centered free radicals are generated during copolymerization of styrene and *n*-butyl acrylate by ATRP.

According to Heuts and Davis,[12] the *relative* radical concentrations in conventional free radical copolymerizations should be the same as those in ATRP copolymerizations. Direct exchange between two active radicals can only occur through cross-propagation reactions, and the exchange reactions in ATRP have no net contribution to the total rates of cross-propagation. Our composition and sequence distribution results are consistent with their interpretation of ATRP copolymerization kinetics.

Conclusions

Atom transfer radical polymerization has been used to simultaneously copolymerize styrene and *n*-butyl acrylate. Kinetic studies indicate an irreversible termination reaction whose contribution can be suppressed at temperatures below 70 °C. Polymerization of styrene in *n*-butyl propionate (a nonpolymerizable model for *n*-butyl acrylate) show termination, indicating that end group stability of polystyrene chain ends may be decreased by the presence of *n*-butyl acrylate in the reaction.

Molecular weight behavior in copolymerizations is consistent with polymerizations proceeding with no transfer and with no radical−radical combination reactions. Differences between theoretical and measured molecular weights show a maximum at around 2.5×10^4 and remain constant with increasing molecular weight, suggesting that the molecular weight dependence of $[\eta]$ (and therefore the hydrodynamic volume) of copolymers are different from polystyrene. Polydispersities in the reactions remain low until higher conversions, where they increase slightly.

Composition versus conversion in statistical copolymers prepared by ATRP can be described by a simple terminal model scheme. Results show that composition is independent of [CuBr], [I], and temperature for $(f_{st})_0 = 0.51$. Monomer reactivity ratios calculated using a nonlinear least-squares method are $0.68 \le r_1 \le 0.82$ and $0.22 \le r_2 \le 0.26$. ^{13}C NMR spectra of copolymers prepared by ATRP are very similar to spectra of copolymers prepared by conventional free radical polymerizations. These results on composition and sequence distribution indicate that carbon-centered free radicals are generated in this metal-catalyzed polymerization.

Acknowledgment. The authors thank the members of the Atom Transfer Radical Polymerization Consortium at Carnegie Mellon University and the Department of the Army (AASERT Contract DAA655-97-1-0191) for support.

Supporting Information Available: Kinetic, molecular weight, and composition data for all copolymerizations presented, kinetic and molecular weight data on polymerization of *n*-butyl acrylate, kinetic data used to determine equilibrium constants, and calculations of reactivity ratios (including the VBA code used to construct the SS space in Excel 7.0). This material is available free of charge via the Internet at http://pubs.acs.org.

References and Notes

(1) Matyjaszewski, K. *Controlled Radical Polymerization*; ACS Symposium Series No. 685; American Chemical Society: Washington, DC, 1997.
(2) Kazmaier, P. M.; Daimon, K.; Georges, M. K.; Hamer, G. K.; Veregin, R. P. N. *Macromolecules* **1997**, *30*, 2228.
(3) Hawker, C. J.; Elce, E.; Dao, J.; Volksen, W.; Russell, T. P.; Barclay, G. G. *Macromolecules* **1996**, *29*, 2686.
(4) Fukuda, T.; Terauchi, T.; Goto, A.; Tsujii, Y.; Miyamoto, T.; Shimizu, Y. *Macromolecules* **1996**, *29*, 3050.
(5) Although the temperature was listed (40 °C), the exact experimental conditions were not given. Presumably, the copolymer was a low-conversion statistical copolymer prepared by AIBN.
(6) Haddleton, D. M.; Crossman, M. C.; Hunt, K. H.; Topping, C.; Waterson, C.; Suddaby, K. G. *Macromolecules* **1997**, *30*, 3992.
(7) Kotani, Y.; Kamigaito, M.; Sawamoto, M. *Macromolecules* **1998**, *31*, 5582.
(8) Arehart, S. V.; Greszta, D.; Matyjaszewski, K. *ACS Polym. Prepr.* **1997**, *38* (1), 705.
(9) Greszta, D.; Matyjaszewski, K.; Pakula, T. *ACS Polym. Prepr.* **1997**, *38* (1), 709.
(10) Greszta, D.; Matyjaszewski, K. *ACS Polym. Prepr.* **1996**, *37* (1), 569.
(11) Pakula, T.; Matyjaszewski, K. *Macromol. Theory Simul.* **1996**, *5*, 987.
(12) Heuts, J. P. A.; Davis, T. P. *Macromol. Rapid Commun.* **1998**, *19*, 371.
(13) Fischer, H. *Macromolecules* **1997**, *30*, 5666.
(14) Stockmayer, W. H. *J. Chem. Phys.* **1945**, *13*, 199.
(15) Hadda, T. B.; Bozec, H. L. *Polyhedron* **1988**, *7*, 575.
(16) Mandel, J. *The Statistical Analysis of Experimental Data*; Dover Publications: New York, 1964; p 36.
(17) Petrak, K. L.; Pitts, E. *Polymer* **1983**, *24*, 729.
(18) Skoog, D. A.; Leary, J. J. *Principles of Instrumental Analysis*; 4th ed.; Saunders College Publishing: Forth Worth, 1992; Appendix 1.
(19) Chujo, R.; Hatada, K.; Kitamaru, R.; Kitayama, T.; Sato, H.; Tanaka, Y. *Polym. J.* **1987**, *19*, 413.
(20) van Herk, A. M.; Dröge, T. *Macromol. Theory Simul.* **1997**, *6*, 1263.
(21) Patino-Leal, H.; Reilly, P. M.; O'Driscoll, K. F. *J. Polym. Sci., Polym. Lett. Ed.* **1980**, *18*, 219.
(22) van Herk, A. M. *J. Chem. Educ.* **1995**, *72*, 138.
(23) Matyjaszewski, K.; Patten, T. E.; Xia, J. *J. Am. Chem. Soc.* **1997**, *119*, 674.
(24) This is available in the Supporting Information.
(25) Matyjaszewski, K.; Davis, K.; Patten, T. E.; Wei, M. *Tetrahedron* **1997**, *53*, 15321.
(26) Plotting DRI/M versus V_e accounts for the mass-sensitive property of the RI detector. This plot gives the same information as plotting DRI/M^2 versus M.
(27) Moad, G.; Solomon, D. H. *The Chemistry of Free Radical Polymerization*; Elsevier: New York, 1995; pp 219, 231.

(28) Matyjaszewski, K.; Coca, S.; Nakagawa, Y.; Xia, J. *ACS PMSE Prepr.* **1997**, *76*, 147.
(29) Matyjaszewski, K.; Nakagawa, Y.; Jasieczek, C. B. *Macromolecules* **1998**, *31*, 1535.
(30) Quirk, R. P.; Lee, B. *Polym. Int.* **1992**, *27*, 359.
(31) Matyjaszewski, K. *Macromol. Symp.* **1996**, *111*, 47.
(32) Kaszás, G.; Földes-Berezsnich, T.; Tüdös, F. *Eur. Polym. J.* **1984**, *20*, 395.
(33) Manders, B. G.; Chambard, G.; Kingma, W. J.; Klumperman, B.; van Herk, A. M.; German, A. L. *J. Polym. Sci., Polym. Chem. Ed.* **1996**, *34*, 2473.
(34) Lyons, R. A.; Hutovic, J.; Piton, M. C.; Christie, D. I.; Clay, P. A.; Manders, B. G.; Kable, S. H.; Gilbert, R. G. *Macromolecules* **1996**, *29*, 1918.
(35) Coote, M. L.; Johnston, L. P. M.; Davis, T. P. *Macromolecules* **1997**, *30*, 8191.
(36) Behnken, D. W. *J. Polym. Sci., Part A* **1964**, *2*, 645.
(37) Tidwell, P. W.; Mortimer, G. A. *J. Polym. Sci., Part A* **1965**, *3*, 369.
(38) Moad, G.; Solomon, D. H. *The Chemistry of Free Radical Polymerization*; Elsevier: New York, 1995; pp 287, 295.
(39) Llauro-Darricades, M. F.; Pichot, C.; Guillot, J.; Rios, L.; Cruz, M. A.; Guzman, C. *Polymer* **1986**, *27*, 889.
(40) Brar, A. S.; Sunita; Satyanarayana, C. V. V. *Polym. J.* **1992**, *24*, 879.
(41) Dube, M.; Sanayei, R. A.; Penlidis, A.; O'Driscoll, K. F.; Reilly, P. M. *J. Polym. Sci., Polym. Chem. Ed.* **1991**, *29*, 703.
(42) Ziaee, F.; Nekoomanesh, M. *Polymer* **1998**, *39*, 203.

MA981693V